



## EXPERIMENTAL INVESTIGATION OF FRP RC SUB-ASSEMBLAGE WITH SMA BAR IN THE PLASTIC HINGE REGION OF BEAM

M. Shahria Alam<sup>1</sup>, Moncef Nehdi<sup>2</sup> and Maged A. Youssef<sup>3</sup>

### ABSTRACT

High corrosion resistance has made Fibre-Reinforced Polymer (FRP) bars increasingly accepted as reinforcement in concrete structures. However, the lack of ductility is a major concern for the use of FRP reinforcement in seismic regions. However, FRP reinforced concrete (RC) structures can be made ductile by utilizing a ductile material such as steel at the plastic hinge regions. However, the use of steel negates the corrosion resistance purpose of FRP. Nickel-Titanium (Ni-Ti) shape memory alloy (SMA) is highly resistant to corrosion and has added advantage in seismic regions since it can undergo large deformation, yet regain its undeformed shape through stress removal. In this study, an FRP RC beam-column joint with SMA bar at the plastic hinge region of the beam is proposed to address both corrosion resistance and seismic related problems. This joint is reinforced with superelastic Ni-Ti SMA bar at the plastic hinge regions of the beam and FRP in the other regions of the beam and column. The performance of the proposed joint is studied under reversed cyclic loading. The results were compared, in terms of load-storey drift, and energy dissipation capacity, to those of the original specimen. Both the original and repaired joints proved to dissipate adequate energy under earthquake type loading. The proposed BCJ is not only corrosion resistant, but can also provide adequate energy dissipation during large earthquakes, therefore mitigating major problems related to infrastructure management.

Keywords: FRP bar, shape memory alloy, superelastic, seismic, energy dissipation.

### Introduction

Steel reinforcements have been used in concrete structure for more than hundred years. Corrosion of steel is a major problem which causes early deterioration of reinforced concrete (RC) structures. A number of bridges have collapsed over the years where corrosion of steel has been identified as a root cause of such failures. Billions of dollars are spent annually for the rehabilitation of civil infrastructure especially for the replacement of corroded steel. Fibre-reinforced polymer (FRP) bars have been introduced as reinforcement for concrete in order to mitigate such corrosion problems. However, FRP is a brittle material and ductility is its main problem for FRP RC structures. Therefore, the use of FRP in RC structures still remains to be of

---

<sup>1</sup>Assistant Professor, School of Engineering, The University of British Columbia, Kelowna, BC V1V 1V7

<sup>2</sup>Professor, Dept. of Civil and Env Engineering, The University of Western Ontario, London, ON, N6A 5B9

<sup>3</sup>Assoc. Professor, Dept. of Civil and Env Engineering, The University of Western Ontario, London, ON, N6A 5B9

great concern, especially, in seismic regions where ductility is one of the most important issues. Again, the absence of yielding and an inelastic branch in the stress-strain behaviour of FRP will result in a sudden and brittle failure without adequate warning. Consequently, such FRP RC elements are often overdesigned in order to avoid rupture of FRP bars and to increase safety of the structure.

Ductility of FRP RC structures can be achieved in conjunction with a ductile material e.g. steel, stainless-steel or shape memory alloy, etc., which will be placed at the plastic hinge regions of a structure, whereas FRP bars will be used in the other regions of the structure. These materials are chosen because of their comparable yield strengths. Due to the corrosion problem, stainless steel can be taken into consideration instead of regular steel. Another option might be the use of shape memory alloy (SMA) bar, which is also highly resistant to corrosion and superelastic (SE). SMA is a unique alloy with the ability to undergo large deformation, but can regain its undeformed shape through stress removal. In the case of using stainless steel along with FRP bars, this can reduce maintenance costs since there will be no significant corrosion. However, if the structure is subjected to an earthquake, the stainless steel will undergo inelastic deformation and will not be able to recover its original shape, thus, will experience permanent deformation. On the other hand, the use of SMA as reinforcement will not only eliminate the corrosion problem, but also allow to recover inelastic deformation at the end of earthquakes. Another advantage is that such structural element can sustain repeated earthquake loading even though the SMA rebar is being strained beyond its yield limit. In contrast, stainless steel will accumulate deformation and lose its serviceability. Nevertheless, stainless steel is currently less costly compared to SMA.

The objective of this study is to investigate the seismic behaviour of a concrete beam column sub-assembly reinforced with SE SMA in its plastic hinge zone and FRP in other regions, and compare its performance to that of a regular steel RC BCJ in terms of load-displacement, and energy dissipation capacity, and strains in the longitudinal reinforcements.

### **Design Philosophy of Beam-Column Joints**

This section talks about the failure mechanism of RC beam-column joint and the new philosophy for designing RC structures and its elements that eventually leads to the use of superelastic SMA as reinforcement. A number of researchers e.g. [Meinheit and Jirsa \(1981\)](#), [Ghobarah and El-Amoury \(2005\)](#) and others devoted significant effort studying the behavior of joints, as well as on the development of design recommendations for ensuring adequate connection behavior in frame structures expected to undergo large inelastic deformations. RC structures are subjected to severe damage and collapse during strong earthquakes. Structures are designed for safety conditions, where earthquake energies are dissipated through yielding of reinforcement and its inelastic deformation resulting in permanent damages. More recently the vision has been broadened where the designers/owners no longer want to surrender their own creations/constructions. The seismic design of structures has evolved towards performance-based design in which there is need for new structural members and systems that possess enhanced deformation capacity and ductility, higher damage tolerance, concrete confinement, decreased or minimized residual crack sizes, recovered and reduced permanent deformations.

The design of ductile moment-resisting frames attempts to force the structure to respond in a strong column-weak beam action in which plastic hinges induced by seismic forces form at the ends of beams. The hinging regions are detailed to allow plastic hinges to undergo yielding in both positive and negative moment, thus ensuring a substantial amount of energy dissipation during earthquakes. If SMA is used as reinforcements instead of steel or FRP in the desired hinge

locations of beams, it will not only be able to dissipate seismic energy, but will also be able to restore its original shape after the seismic event by heating (through shape memory effect) or simply upon stress removal (through superelasticity). Because of its higher cost compared to other construction materials, SMA longitudinal rebars will be used along with FRP rebars, and SMAs are placed particularly in the hinge regions of beams. If such a RC beam-column joint can be built, this will allow structural engineers to design connections for longer service life with no possible corrosion, particularly in seismic regions this will exhibit little damage during earthquake eliminating post earthquake joint repairs (Parra-Montesinos et al. 2005).

### FE Program for Analyzing Beam-Column Joint

In the present paper several inelastic time-history analyses have been performed to predict the performances of RC structural elements using a FE program. Fiber modelling approach has been employed to clearly represent the distribution of material nonlinearity along the length and cross-sectional area of the member. 3D beam-column elements have been used for modelling the beam and column where the sectional stress-strain state of the elements is obtained through the integration of the nonlinear uniaxial stress-strain response of the individual fibers in which the section has been subdivided, completely following the spread of material inelasticity within the member cross-section and along the member length. Concrete and steel has been modelled using models of Martinez-Rueda and Elnashai (1997) and Monti and Nuti (1992), respectively. SMA has been modelled according to the model of Auricchio and Sacco (1997). Figure 1 shows the 1D-superelastic model used in the FE program where SMA has been subjected to multiple stress cycles at a constant temperature and undergoes stress induced transformation. The parameters used to define the material model are: 1)  $f_y$ ; 2)  $f_{P1}$ ; 3)  $f_{T1}$ ; 4)  $f_{T2}$ ; 5) superelastic plateau strain length,  $\epsilon_l$  and 6) modulus of elasticity,  $E$ .

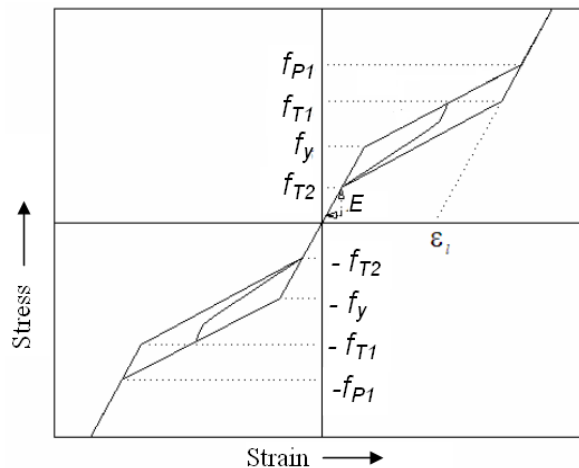


Figure 1. 1-D-Superelastic model of SMA (Auricchio and Sacco 1997)

#### Validation of the Program

Before using this program in predicting the performance of the SMA-steel- and steel-RC beam-column joint, it is important to first verify the FE program with some experimental results. For validation purposes two cases have been taken into consideration as described in the following section.

#### Case 1: Steel-RC Joint

Said and Nehdi (2004a) tested a full-scale RC beam-column joint designed as per the CSA A23.3-

94 (1994) requirements under reversed cyclic load. A FE mesh has been developed for the beam-column joint where the geometry, material properties are made according to the experimental work of Said and Nehdi (2004a) and subjected to similar kind of loading. Then the FE program has been used to solve the inelastic static time-history analysis. Figure 2a and 2b present the experimental and numerical results of the tested specimen, respectively showing the beam tip load versus beam tip displacement up to its ultimate load. The ultimate beam tip load of the FE model was predicted as 127 kN at a tip displacement of 141 mm compared to that of the experimental results where the tip load was 138 kN at a tip displacement of 143 mm. The total energy dissipation up to its ultimate load of the FE model was calculated as 131 kN.m, which is 13% smaller compared to that of the experimental results. Concrete crushing and yielding of reinforcement was observed in the FE model similar to that of the tested specimen. The numerical results show that the FE program is capable of predicting the behavior of the joint with reasonable accuracy.

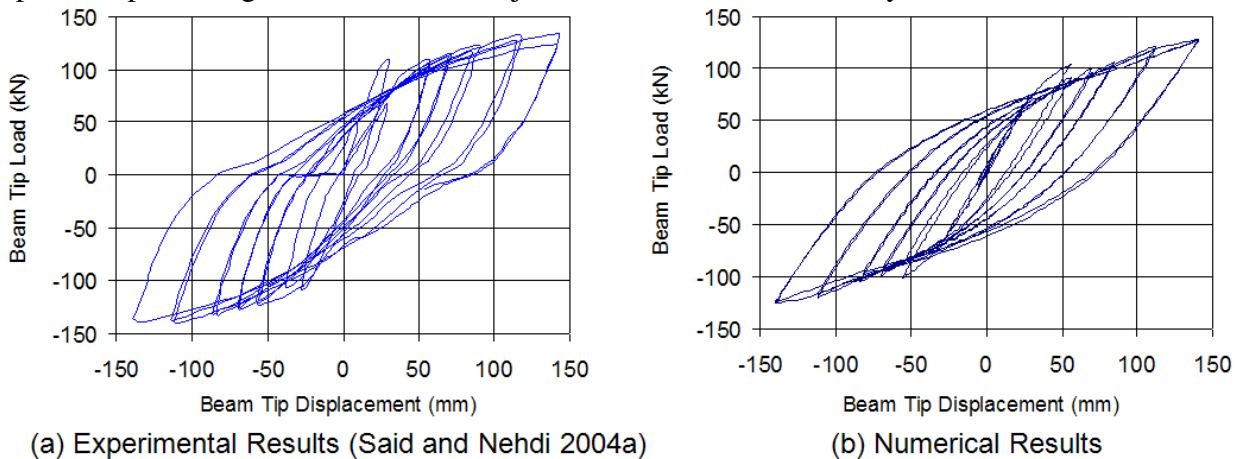


Figure 2. Beam tip-load vs tip-displacement for steel-RC BCJ under reversed cyclic loading.

### Case 2: SMA-Steel-RC Joint

Two quarter-scale spiral RC columns representing RC bridge piers were designed, constructed and tested using a shake table by [Saiidi and Wang \(2006\)](#). The bridge pier was reinforced with SMA rebars placed at the plastic hinge region and connected to the steel rebars with mechanical couplers. Figure 3a shows the experimental results of the bridge pier with excellent recentering capability when subjected to base acceleration. An inelastic dynamic analysis has been performed using the FE program to predict the performance of the bridge pier tested by [Saiidi and Wang \(2006\)](#). SMA has been modelled according to Fig. 1. Figure 3b depicts the predicted base shear-tip displacement of the numerical model which seems to be fairly accurate as compared to the experimental results shown in Fig. 3a. The maximum base shear and the tip displacement were predicted as 81.5 kN and 62.0 mm compared to experimental values of 77.2 kN and 66.0 mm, respectively. The numerical results predicted by the model show good agreement with the experimental results which varies by only 5.6% for base shear and 6.1% for tip displacement. The accumulated energy dissipation was calculated as 48.2 kN.m from the predicted load-displacement curve where as the amount of energy dissipation obtained from the experimental result was 44.0 kN.m, which is only 9.4% lower than the calculated result. The SMA-steel-RC column failed by concrete crushing and yielding of SMA rebar within superelastic strain range and the displacement ductility was measured as 5.9, whereas in the numerical analysis, the model also failed due to crushing of concrete and yielding of SMA within superelastic strain limit with a displacement ductility of 6.7.

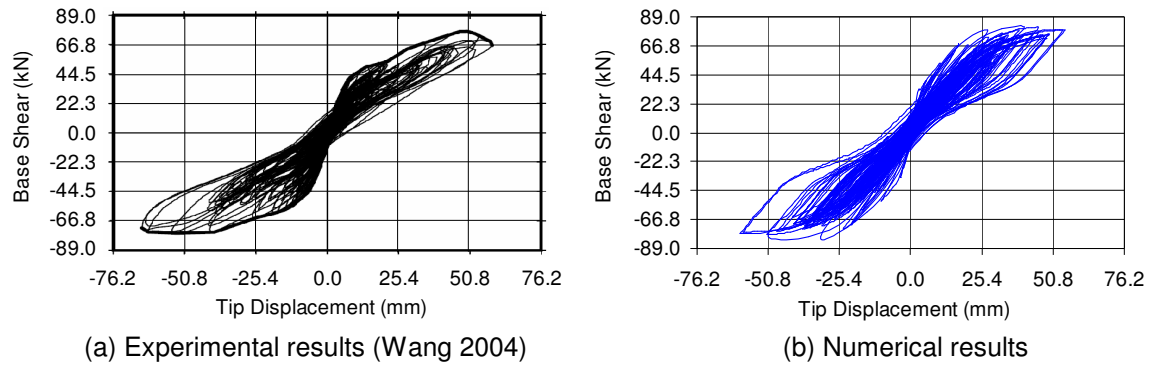


Figure 3. Base shear versus tip-displacement for SMA-steel-RC bridge pier under earthquake type loading.

### Model Description and its Component Design

It has been observed that medium rise buildings are more susceptible to damage during an earthquake (Bariola 1992). Hence, a medium rise regular RC moment resisting frame building with eight storey has been selected in this study to investigate the performance of its exterior beam-column joint of a particular storey. The building has been designed and detailed in accordance with Canadian Standards (CSA A23.3-04). The building is assumed to be located in the western part of Canada on firm ground with un-drained shear strength more than 100 kPa (soil class C, NBCC 2005). The elevation and plan of this building is shown in Fig.4. Here, the building is composed of equal storey heights of 4.00 m with equal column spacing of 4.85 m in both directions. The building is designed with moderate level of ductility (seismic force reduction factor of 2.5).

An exterior beam-column joint has been isolated at the points of contraflexure from the mid-height of fifth floor to the mid-height of sixth floor measuring 4 m in height (abcd in Fig. 4a) by 2.93 m in length taken from the exterior bay to its mid-span (abcd in Fig.4a and efgh in Fig.4b). It is to be noted that this study is a part of an experimental project which will investigate the performance of this exterior beam-column joint in the laboratory. The present study is conducted to predict the experimental results prior to testing. Depending on the laboratory space and equipment limits, the size of the test specimens has been scaled down to  $\frac{3}{4}$ . The forces acting on the joints were also scaled down by a factor of  $(\frac{3}{4})^2$ . This factor has been chosen to maintain the stresses in the scaled models similar to the full-scale joint.

Two beam-column joint specimens will be taken into account. The detailed design is the same for both the joints except, one will be reinforced with regular steel bar all through (specimen JBC-1), while the other will be reinforced with SMA at the plastic hinge region of the beam and FRP bars in the remaining portion of the joint (specimen JBC-2). The detailed design of the joint (JBC-1 and JBC-2) is shown in Fig.5. The material properties used in the program are presented in Table 1. The beam and the column have been designed with the maximum moment and shear forces developed during the analysis of the building considering all possible combinations of load cases suggested by the building code. The column axial force, P has been taken from the analysis of the corresponding load case for which the column has been designed and is found originally as 620 kN, after scaling down P becomes 350 kN. The reduced cross section of the column is chosen as 250 x 400 mm with 4-M20 longitudinal rebars corresponding to a 1.2% reinforcement ratio (M20 is equivalent to 19.5 mm diameter steel bar and 19.05 mm diameter GFRP bar). The column

is transversely reinforced with M10 (11.3 mm diameter steel bar and 10 mm diameter GFRP bar) closed rectangular ties. The closed ties are also placed in the joint with 80 mm c/c spacing. The column ties were spaced at 80 mm along 640 mm above and below the face of the joint and then spaced at 125 mm for the rest of the column's height.

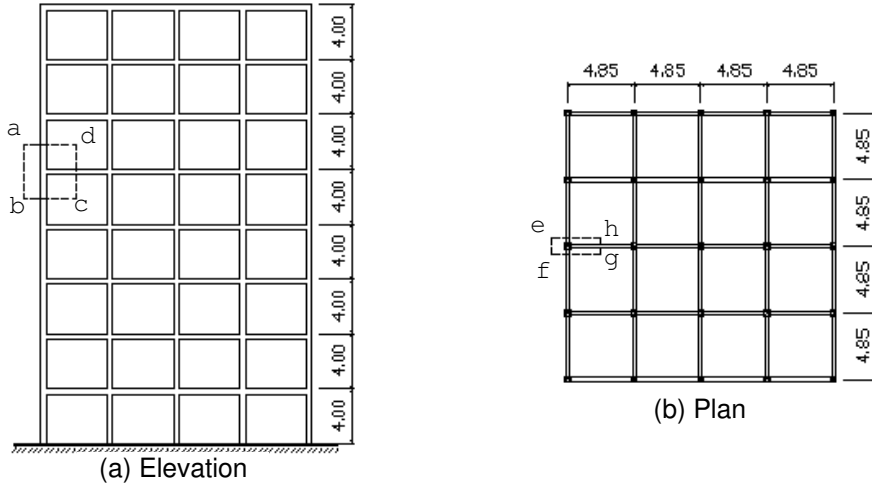


Figure 4. 8-storey frame building a) elevation and b) plan.

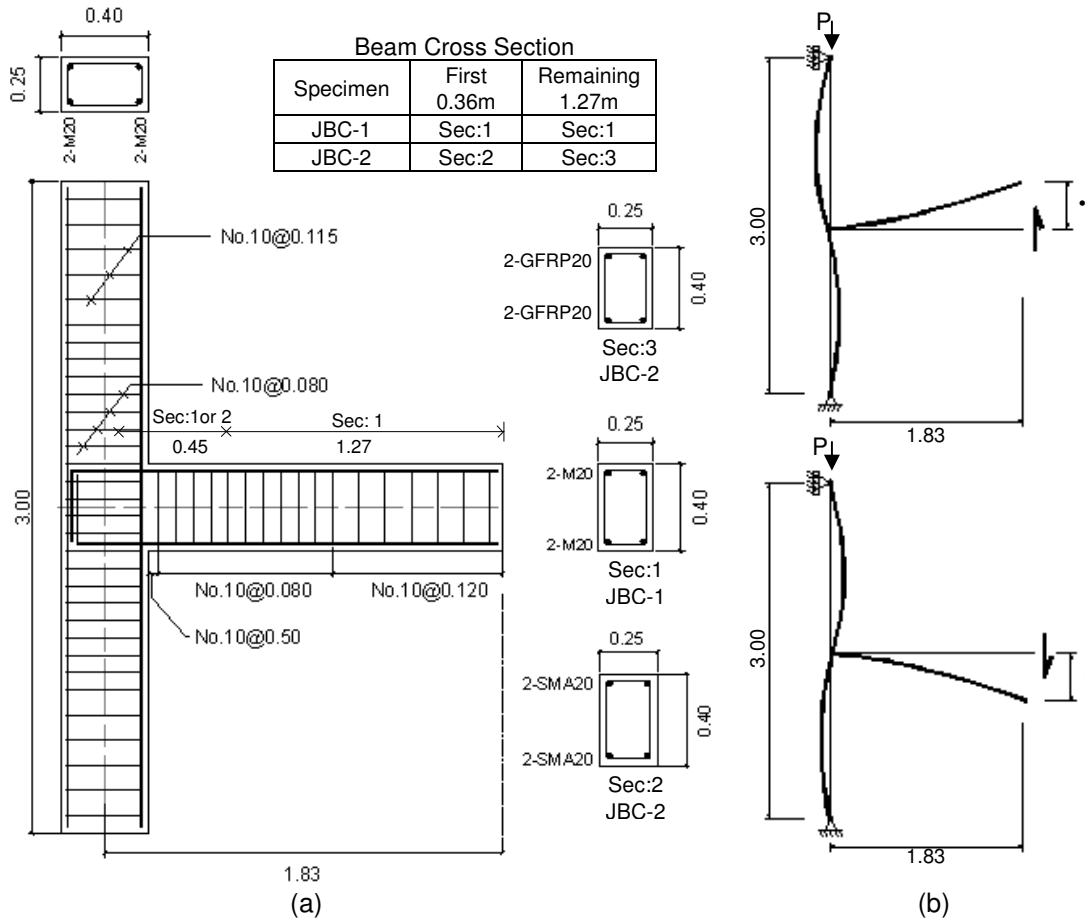


Figure 5. (a) Reinforcement details of specimen JBC-1 and JBC-2, (b) typical deflected (m).

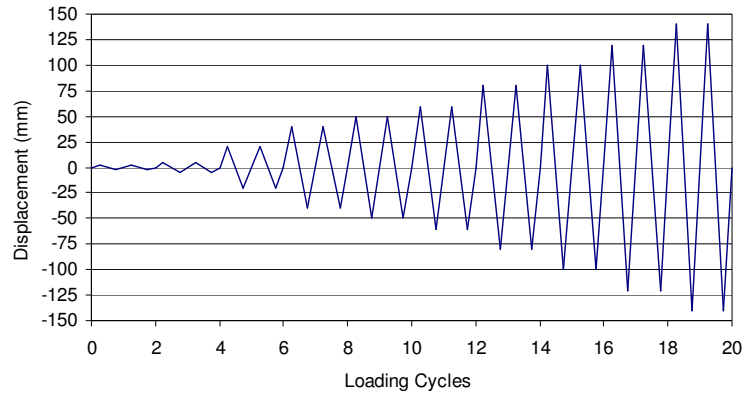


Figure 6. Reversed cyclic loading sequence used in this study.

Table 1: Material properties used in the FE program

Material	Property	Value
Concrete	Compressive strength (MPa)	50.9
	Strain at peak stress (%)	0.18
	Modulus of Rupture (MPa)	4800
M20 Steel	Yield Strength (MPa)	500
	Strain hardening parameter (Post yield stiffness/initial stiffness)	0.03
M10 Steel	Yield Strength (MPa)	450
GFRP20	Modulus of elasticity, $E_{GFRP}$ (MPa)	47600
	Ultimate tensile strength (MPa)	728
SMA20	Modulus of elasticity, $E_{SMA}$ (MPa)	64000
	$f_y$ as in Fig. 1 (MPa)	400
	$f_{P1}$ as in Fig. 1 (MPa)	510
	$f_{T1}$ as in Fig. 1 (MPa)	370
	$f_{T2}$ as in Fig. 1 (MPa)	225
	$\epsilon_l$ as in Fig. 1 (%)	6.00

The top and bottom longitudinal reinforcements of the beam of specimens JBC-1 and JBC-2 at the plastic hinge regions are 2-M20 bars and 2-SMA20 bars (SMA20 is equivalent to 20.6 mm diameter bar) corresponding to 1.2% and 1.5% reinforcement ratio, respectively (Fig. 5a). For both specimens, the first transverse reinforcement (M10 closed rectangular tie) of the beam was placed 50 mm from the face of the column. Then the ties were spaced at 80 mm for the 800 mm of the beam adjacent to the column (equivalent to twice the beam's depth) and then spaced at 120 mm for the remaining of the beam. The size of longitudinal rebar and the size and spacing of the transverse reinforcement for the joint and hinging zones confinement satisfactorily conform to the current code requirements. The specimen satisfies an adequate beam to column strength ratio as suggested by the current CSA design code.

The geometry, longitudinal and transverse reinforcement arrangements of the columns are the same for both the specimens. In case of beam, JBC-1 and JBC-2 are the same in terms of geometry, and transverse reinforcement and its arrangement; the only difference in JBC-2 is the use of SMA as longitudinal reinforcement instead of regular steel (JBC-1) at its plastic hinge region where the plastic hinge length is calculated as 360 mm (Paulay and Priestley 1992) for JBC-2 from the face of the column. Mechanical couplers will be used to connect SMA whereas epoxy adhesive will be used to connect FRP rebar with the coupler. While couplers are being placed inside the joint, the total length of SMA bar becomes 450 mm from the centre to centre of

the coupler as shown in Fig. 5a. Figure 5b shows the idealized support conditions and typical deflected shape of the joint under reversed cycles of tip-displacement.

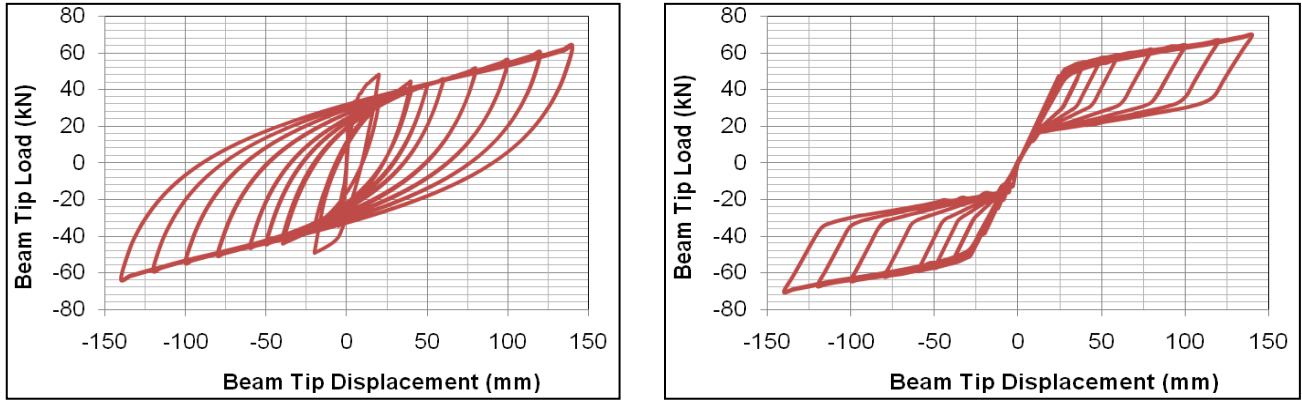


Figure 7. Beam tip load-displacement relationship for the (a) steel-RC beam-column joint (JBC-1), (b) SMA-FRP-RC beam-column joint (JBC-2).

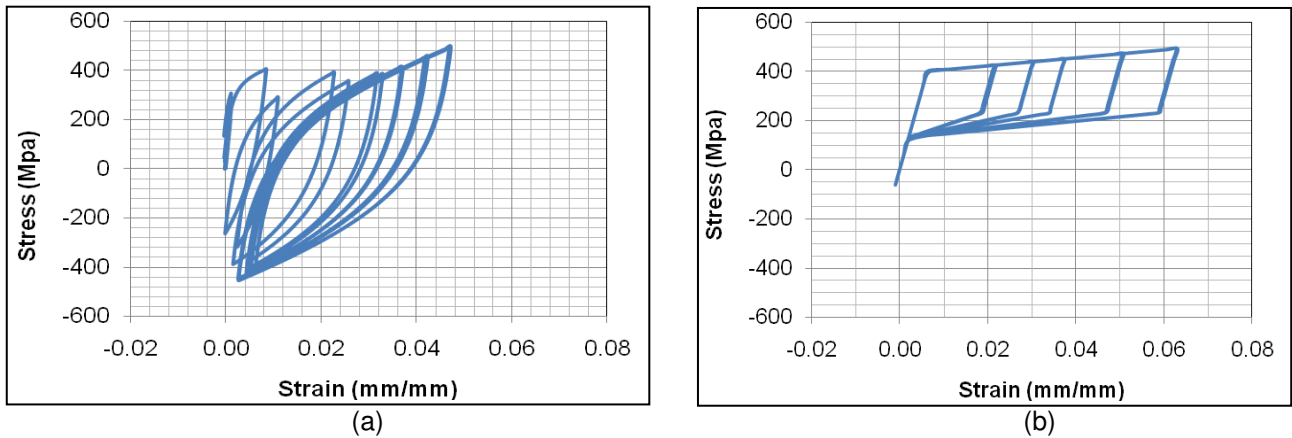


Figure 8. Stress-strain relationship for the (a) steel-RC beam-column joint (JBC-1), (b) SMA-FRP-RC beam-column joint (JBC-2).

## Results and Discussions

The two exterior beam-column subassemblages JBC-1 and JBC-2 are analyzed under reversed cyclic displacements. Displacement controlled loading cycle is applied at the beam-tip with the sequence shown in Fig. 6. Figure 7a and 7b show the load-deflection curves for specimen JBC-1 and JBC-2, respectively. In case of JBC-1, the first flexural crack was observed at a load of 21 kN. The top steel yielded at a load of 39.6 kN and the bottom steel yielded at 40.9 kN load. The maximum load was found as 63.8 kN in the whole load cycle. Figure 8a show the strain measurements close to the column face in the beam main top steel reinforcing bar. It can be observed from the force-displacement relationship of JBC-1 (Fig. 8a) that when the force drops to zero there was large residual displacement at the beam-tip (89 mm) with significant amount of strain at beam rebars at the column face (Fig. 8a). In case of JBC-2, the first flexural crack was observed at a load of 18.7 kN. The top SMA yielded at a load of 49.5 kN and the bottom SMA yielded at a load of 47.0 kN. However, the maximum load was found to be 70.6 kN in the whole loading cycle. In the second specimen, the exterior concrete of the beam close to the column face started crushing and spalling off at a load of 64.0 kN. As the load continued, the joint started to

produce larger loads with the core concrete still within the limiting range of crushing strain. Figure 8b show the stress-strain measurements close to the column face in the beam main top SMA reinforcing bar. Both the diagrams show flag shaped response under tension and almost linear response under compression since concrete contributed substantial portion under compression and thus, reducing the demand on SMA rebars. The force-displacement relationship of JBC-2 shows that there will be a very small amount of residual displacement (1.8 mm) at the beam tip at zero force which is due to almost zero strain in SMA rebar (Fig.8b).

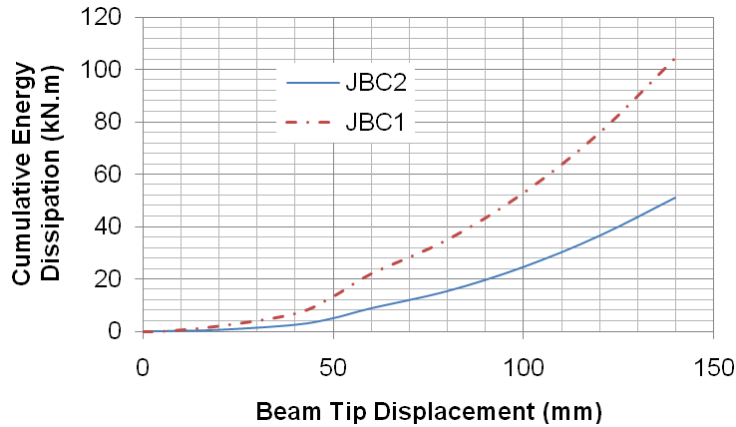


Figure 9. Cumulative energy dissipation capacity of JBC-1 and JBC-2

Figure 9 shows the cumulative energy dissipation by JBC1 and JBC2. The amount of energy absorbed by JBC-1 was found as 104 kN.m whereas by JBC-2 was 51 kN.m. The results show that JBC-2 dissipated 50% less energy compared to JBC-1, i.e. the conventional steel-RC beam-column joint showed better performance in energy dissipation capacity because of its large hysteretic loop. The model does not account for slippage of SMA and FRP bars inside the coupler, which

would have increased the energy dissipation capacity of JBC2. The advantage of SMA-FRP-RC beam-column joint lies in its corrosion resistance and especially, its recentering capability even after large displacements. This proves JBC-2 a better option compared to JBC-1 in earthquake resistant RC frame structures and corrosive environment, which will be able to dissipate significant amount of energy during an earthquake by undergoing large displacements but potentially recover all of its deformation after the earthquake requiring minimum amount of repairing and also, it will not require any maintenance in a corrosive environment compared to regular RC structures.

There is a significant difference between SMA and steel in its modulus of elasticity where the modulus of elasticity of SMA is only 1/3 of steel modulus used in the specimens. The yield strength of SMA and steel were also different which were 400 and 500 MPa, respectively. Therefore, the diameter of SMA rebar was taken a bit higher (20.6 mm) compared to that of steel diameter (19.5 mm). The concrete compressive strength was the same for both the specimens. There was another difference in the geometry in cross-section. Due to the presence of couplers in JBC-2, the effective depth was 10 mm lesser than that of JBC-1. This led to the development of an early crack in JBC-2 compared to that of JBC-1 showing low cracking moment. The concrete clear cover was considered as 17 mm for both specimens. All these differences make it less critical in direct comparison of the beam-column joint responses of specimens JBC-1 and JBC-2 except the qualitative load-deflection hysteretic curves.

## Conclusions

This paper discusses a novel approach to reduce the seismic vulnerability of RC structures by utilizing smart materials like SMA and FRP in beam-column elements. The objective of this study is to investigate the cyclic performance of an exterior beam-column joint which has been isolated from an eight-storey building located in high seismic zone of western part of Canada. This joint

specimen has been designed according to CSA standards (A 23.3-04) in two ways: one with regular steel rebar (Specimen JBC-1) and the other with superelastic SMA rebar (Specimen JBC-2) at its plastic hinge region and FRP in other regions. Both specimens JBC-1 and JBC-2 have been analyzed under cyclic displacement loading with the use of a finite element program and their performances have been compared. Before analyzing the beam-column joints, the FE program has been validated by the experimental results of beam-column joint reinforced with regular steel (Said and Nehdi 2004a) and a column-foundation joint reinforced with SMA-steel coupled reinforcement at its plastic hinge location. Both the numerical results indicate that the FE program can predict the hysteretic load-displacement curve with reasonable accuracy.

The analytical results of the hysteretic load-displacement curves of JBC-2 exhibited better performance compared to that of JBC-1 in terms of residual displacements remaining in the joint after unloading. The flag-shaped stress-strain hysteresis of superelastic SMA bars produced flag-shaped hysteretic load-displacement curves in the SMA-steel-RC beam-column joint (JBC-2). Although steel-RC beam-column joint (JBC-1) dissipated higher amount of energy compared to that of JBC-2 because of its large hysteretic loops, still JBC-2 performed better because of its capability in recovering post-elastic strain, which makes it very attractive in high seismic regions where the beam-column joints will be able to dissipate significant amount of energy and remain functional even after a strong earthquake. Another major advantage is that the FRP-SMA RC BCJ is highly resistant against corrosion. If SMA can be used as reinforcement in beam-column joints, it can initiate major progress in seismic design whereby the repair cost may be substantially reduced and the structure may remain serviceable even after a severe earthquake.

## References

- Auricchio, F. and Sacco, E., 1997. Superelastic shape-memory-alloy beam model, *Journal of Intelligent Material Systems and Structures*, 8(6), 489-501.
- Bariola, J., 1992. Drift response of medium-rise reinforced concrete buildings during earthquakes, *ACI Structural Journal*, 89(4), 384-390.
- Design of Concrete Structures*, CSA A23.3-04, Canadian Standards Association, Rexdale, Ontario, Canada, 2004, 240p.
- Ghobarah, A., and El-Amoury, T., 2005. Seismic rehabilitation of deficient exterior concrete frame joints, *Journal of Composites for Construction*, 9(5), 408-416.
- Martinez-Rueda, J.E., and Elnashai, A.S., 1997. 1997. Confined concrete model under cyclic load, *Materials and Structures*, 30(3), 1997, pp. 139-147.
- Meinheit, D. F., and Jirsa, J. O., 1981. Shear Strength of RC Beam-Column Connections, *Journal of Structural Division, ASCE*, 107(ST. 11), 2227-2244.
- Monti, G., and Nuti, C., 1992. Nonlinear cyclic behaviour of reinforcing bars including buckling, *Journal of Structural Engineering*, 118(12), 3268-3284.
- National Building Code of Canada, 2005, National Research Council, Canada.
- Parra-Montesinos, G.J., Peterfreund, S.W., and Chao, S., 2005. Highly Damage-Tolerant Beam-Column Joints Through Use of High-Performance Fiber-Reinforced Cement Composites, *ACI Structural Journal*, 102(3), 487-495.
- Said, A.M., and Nehdi, M.L., 2004. Use of FRP for RC Frames in Seismic Zones: Part I. Evaluation of FRP Beam-Column Joint Rehabilitation Techniques, *Applied Composite Materials*, 11(4), 205-226.
- Saiidi, M. S., and Wang, H., 2006. Exploratory study of seismic response of concrete columns with shape memory alloy reinforcement, *ACI Structural Journal*, 103(3), 436-443.